ACS APPLIED MATERIALS & INTERFACES

Research Article

Cite This: ACS Appl. Mater. Interfaces 2019, 11, 4393−4398

www.acsami.org

# Chemical Detection Using a Metal−Organic Framework Single Crystal Coupled to an Optical Fiber

Chen Zhu,[†,‡] Jason A. Perman,[§,‡] Rex E. Gerald, II,[†] Shengqian Ma,[*,§] and Jie Huang[*,†]

[†]Department of Electrical and Computer Engineering, Missouri University of Science and Technology, Rolla, Missouri 65409 United States

[§]Department of Chemistry, University of South Florida, 4202 East Flower Avenue, Tampa, Florida 33620, United States

**ABSTRACT:** The quantitative detection and real-time monitoring of target chemicals in the liquid phase are made possible by combining the tailored adsorption properties of metal−organic framework (MOF) material and the precise measuring capabilities of an optical fiber (OF) Fabry−Pérot interferometer (FPI) device. As the single-crystal MOF host adsorbs target analyte guests from the environment, its dielectric properties change causing the reflection spectrum derived from the FPI device to shift. A single crystal of HKUST-1 was attached to the end-face of an OF to form the sensor OF∪MOF (∪, union). The sensor's response curve was accurately measured using low concentrations of the target analyte nitrobenzene, an explosive simulant. Additionally, the uptake rate of nitrobenzene into the MOF single crystal was characterized. The experimental results show that the sensor achieved quantitative and real-time adsorption measurements of a target analyte.

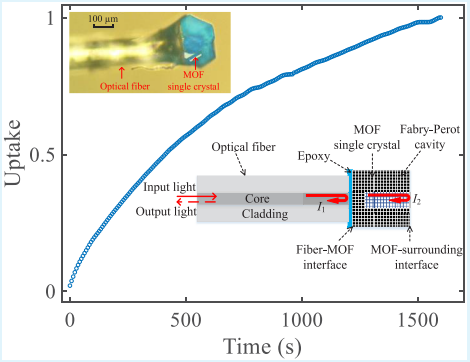


**KEYWORDS:** *optical fiber sensor, metal−organic framework, single crystal, chemical sensor, Fabry−Pérot interferometer, host, guest*



## 1. INTRODUCTION

Rapid, precise, and sensitive detection of target chemicals is essential in many venues of our daily activities, including environmental monitoring of water quality, $O_3$, $CO_2$, antihealth agents, and harmful or dangerous materials combined with benign substances at airport checkpoints.[1−4] To achieve real-time and repetitive detection of multiple target chemicals in different environments that are accessible or inaccessible because of hazardous conditions, optical spectroscopy methods relying on optical fibers (OFs) have been deployed to overcome some of these hurdles.[5] OF sensors offer many advantages over metal-based sensor systems, such as immunity to electromagnetic interferences, remote operation without electricity, high thermal/chemical stability, and distributed sensing platforms.[5−7] However, for measurements of target chemicals, OFs configured for sensing require structurally and chemically designed coatings to extract analytes from their environments. Such coatings have included zeolites, polymers, and metal−organic frameworks (MOFs), with the former showing limited selectivity besides size recognition.

MOFs are extensively used in the areas of separations, storage, and sensing of molecules because their internal physical and chemical properties can be tailored for these applications using the judicious selection of inorganic and organic building blocks.[8−13] These porous frameworks act as chemical hosts and have a unit cell size scale in the angstrom to nanometer range, making it challenging to detect a response from an individual pore within the material. The most promising and effective methods for signal transduction using MOFs for chemical sensing appear to adopt a macroscopic perspective, whereby changes in the material sample as a whole are measured.[14−17] Several kinds of signal transduction schemes for MOF chemical sensors have been proposed.[18] These include optical,[19,20] electrical,[21] and mechanical methods.[22,23] For instance, Achmann et al.[21] reported a means of gas sensing by measuring a MOF's electrical properties when coated on an interdigital electrode. However, the majority of MOFs are not electrical conductors, limiting their sensing applications using this method of signal transduction. For mechanical sensors, MOF thin films have been deposited on surfaces, such as microcantilevers or quartz crystals, whereby changes in the loaded MOF's mass are converted into signals derived from mechanical resonances. Optical transduction methods have also been implemented for MOF sensors, in which MOF thin films are coated on the surface of silicon or plasmonic substrates. These sensors function on the basis of interferometry,[19] LSPR spectroscopy,[20] or luminescence.[24] Researchers have demonstrated high-sensitivity NIR gas sensing for carbon dioxide using Cu-BTC (aka HKUST-1)-coated single-mode and multimode OF,[25,26] or UV-band optical absorption spectroscopy using an etched OF coated with a thin layer of ZIF-8.[27] Additionally, Hromadka et al. proposed an OF long period grating based chemical vapor sensor using ZIF-8 as the functional coating,[16]

Received: November 10, 2018
Accepted: January 2, 2019
Published: January 2, 2019




DOI: 10.1021/acsami.8b19775
ACS Appl. Mater. Interfaces 2019, 11, 4393−4398

or where the end-face of an OF probe was coated with UiO-66 to detect Rhodamine-B.[28]

This precedence of modifying OFs with MOFs for sensing applications has prompted us to design a system that not only monitors the adsorption process of an industrial, environmental, biological, or hazardous chemical but also quantifies its concentration. The sensing mechanism is based on the adsorption of guest molecules that causes changes in the index of refraction of the loaded MOF materials and employs an OF Fabry−Pérot interferometer (FPI) to interrogate those changes.[29,30] In the experimental demonstrations described below, changes in the refractive index response to the presence of nitrobenzene, an explosive simulant, were monitored by attaching a single crystal of HKUST-1 to the end-face of an OF using epoxy. The analyte loadings were quantified by analyzing the shifts of the interference spectra derived from the FPI. Also, the time profile of the uptake process of nitrobenzene in the MOF single crystal was characterized by the OF sensor OF∪MOF (∪, union) and the spectrum analyzer system.

## 2. SENSOR FABRICATION AND MEASUREMENT PRINCIPLE

**Materials.** The materials used to synthesize HKUST-1 were purchased from Sigma Aldrich, including $Cu(NO_3)_2 \cdot 2.5H_2O$, 1,3,5-benzenetricarboxylic acid ($H_3BTC$), *N*,*N*-dimethylformamide (DMF), and $HNO_3$. A Corning SMF-28e single-mode OF, typically used for telecommunication applications, was used to fabricate the sensor. The epoxy used was DEVCON Home 5 Minute Epoxy.

**Sensor Fabrication.** Large single crystals (>0.001 $mm^3$) of HKUST-1 were prepared according to the report by Li et al.,[31] whereby 593 mg (2.55 mmol) of $Cu(NO_3)_2 \cdot 2.5H_2O$ was dissolved in 15 mL of DMF; separately, 422 mg (2.0 mmol) of $H_3BTC$ was dissolved in 10 mL of DMF. Three milliliters of the copper nitrate solution were added to 2 mL of the carboxylic acid solution and slightly stirred before the addition of 20 mL of 2.0 M $HNO_3$. The container was sealed and placed in a freezer for 24 h prior to being placed in an oven set at 85 °C for 7 days, undisturbed. After 7 days, large blue single crystals were visible. The mother liquor was then decanted and exchanged with ethanol three times daily for 3 days to remove unreacted reagents and DMF. The sensor was made by attaching a single crystal of HKUST-1 on the cleaved end-face of the Corning SMF-28e single-mode fiber using a thin layer of epoxy. Then, the sensor was left in air overnight until the epoxy cured.

**Working Principle.** The HKUST-1 crystal structure reveals windows (9 by 9 Å) large enough to accommodate molecules of nitrobenzene (approximate diameter of 4.4 Å).[32] The interactions between HKUST-1 and nitrobenzene are multifold as the oxygens from the nitro group can coordinate with the Cu(II) cation in the HKUST-1 structure,[33] or the aromatic components can stack in face-to-face (slipped) or end-to-face motifs with the $BTC^{3-}$ ligands in the MOF.[34,35]

The sensor consists of an OF and an MOF single crystal (OF∪MOF) attached to the end-face of the OF, as illustrated in the schematic diagram in Figure 1a and the optical microscope image of an OF∪HKUST-1 in Figure 1b. An FPI is formed by the OF−MOF interface and the MOF−surrounding interface, with the MOF crystal acting as the medium of the Fabry−Pérot cavity. The input light transmitted via the core of the OF is partially reflected ($I_1$) by the OF−MOF interface, and the remaining input light that passes

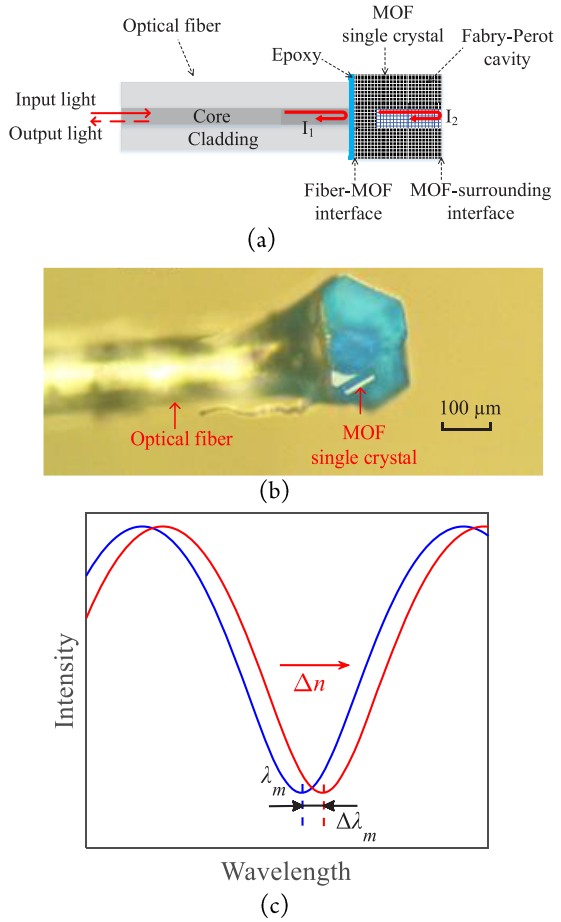


**Figure 1.** (a) Schematic diagram of the OF∪MOF sensor. (b) An optical microscope image of a prototype OF∪MOF sensor. (c) Illustration of a section of the original (blue) and shifted (red) interferograms.

through the crystal is again partially reflected ($I_2$) by the MOF−surrounding interface. These two reflected light beams interfere to generate the output interference signal. The intensity of the interference signal ($I$) is given by

$$I = I_1 + I_2 + 2\sqrt{I_1 I_2}\cos\left(\frac{4\pi nL}{\lambda} + \varphi\right) \quad (1)$$

where $\lambda$ is the optical wavelength of the probe light in vacuum, $\varphi$ is the initial phase difference of the interfering beams, $n$ is the refractive index of the cavity medium (composed of the target analyte guest and the MOF host), and $L$ is the physical length of the cavity. Note that, because a thin layer of epoxy is involved in the sensor design, an additional reflected light beam at the epoxy−MOF interface is introduced, thus modulating the two-beam interferogram (i.e., sinusoidal function). However, the additional modulation will not physically change the sensor's response such that the two-beam interference model is still applicable to the proposed OF∪MOF sensor. When the phase difference between the two partially reflected light beams ($I_1$, $I_2$) satisfies the phase matching condition, a destructive interference pattern is obtained, as shown in Figure 1c, and the wavelength values for the valleys are given by

$$\frac{4\pi nL}{\lambda_m} = (2m + 1)\pi \quad (2)$$



DOI: 10.1021/acsami.8b19775
ACS Appl. Mater. Interfaces 2019, 11, 4393−4398

where $m$ is an integer ($m$ = 1, 2, 3, ...) and $\lambda_m$ is the wavelength of the $m$th-order valley. When the refractive index of the cavity medium changes, the interference spectrum shifts, as schematically illustrated in Figure 1c. The relationship between the shift in the wavelength of a valley ($\Delta\lambda_m$) and the corresponding change in the refractive index ($\Delta n$) is given by:

$$\frac{\Delta\lambda_m}{\lambda_m} = \frac{\Delta n}{n} \tag{3}$$

As can be seen from eq 3, the shifts in the wavelengths of the corresponding valleys are proportional to the changes in the refractive index of the cavity medium. Because most of the MOF's volume consists of open pores, when these pores adsorb analyte guests from the surroundings, there will be a large increase in the loaded MOF's refractive index. Consequently, the responses from all the pores are summed and averaged to produce dielectric changes to the whole MOF volume. The changes in the dielectric properties of the equilibrated guest/host system caused by the adsorption of guest molecules within the porous MOF host can, in turn, be utilized to measure the temporal process of guest adsorption and determine the concentration of the guests in the host at any time. The changes in the refractive index can be precisely determined through an optical interference method by monitoring shifts of the reflection spectra derived from the FPI.

## 3. EXPERIMENTS AND DISCUSSION

Figure 2 schematically shows the system configuration of the OFUMOF for measurements of the adsorption of target chemical

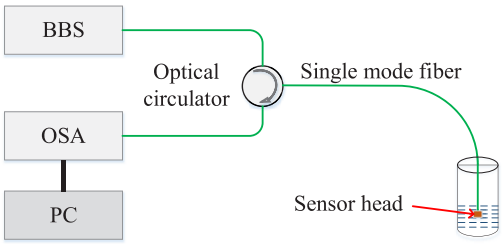


**Figure 2.** Schematic diagram of the experimental setup for the OFUMOF sensor and spectrum analyzer based demodulator system.

guests. A broadband light source (BBS, THORLABS, ASE-FL6002-C4) was employed as the light source. The input light is coupled to the OFUMOF by an optical circulator, which also redirects the OFUMOF modulated signal to an optical spectrum analyzer (OSA, ANDO, AQ6317B). A personal computer (PC) was connected to the OSA through a GPIB cable for data acquisition. Data analysis was performed by a MATLAB program written in-house.

FFT was applied to the reflection spectrum (interferogram) to analyze the light paths in the sensor structure composed of the OFUMOF sensor and OSA recorder system (see Figure 3). The inset of Figure 3 is the reflection spectrum. Multiple optical paths were revealed, as indicated by the several peaks in the FFT plot (spatial domain). The first three relatively large peaks indicate the three main optical paths, that is, through the epoxy layer, through the MOF crystal, and through the epoxy layer and the MOF crystal combined. Although the multiple light beam interferences lead to multimode interference patterns (i.e., not sinusoidal), they do not influence the sensor's performance. Before characterizing the chemical sensing properties, the fabricated OFUMOF sensor was left in air for 2 days to investigate the stability of the MOF single crystal. It was found that only a very small shift in the spectrum was observed, indicating reliable stability of the OFUMOF sensor over a 2 day period of time.

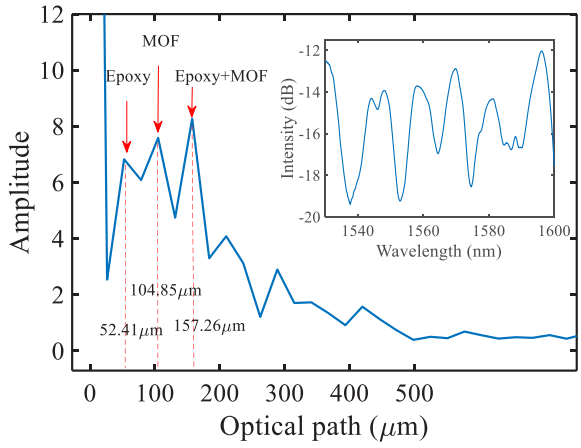


**Figure 3.** FFT of the interference spectrum derived from the OFUMOF sensor and demodulator system. The interference spectrum is shown in the inset. The FFT plot reveals multiple reflections of the incident light in the spatial domain because of the multiple interfaces (e.g., OF|epoxy; epoxy|MOF; MOF|air).

However, long-term performances of the sensor might suffer because of the degradation of the porous structure of the MOF single crystal. Detailed investigations need to be conducted.

The performance of the OFUMOF sensor and demodulator system for quantitative chemical sensing was investigated by immersing the probe in ethanol solutions containing different concentrations of nitrobenzene and recording the corresponding temporal responses. Figure 4 shows the spectral shifts (i.e., the shifts in the wavelengths of

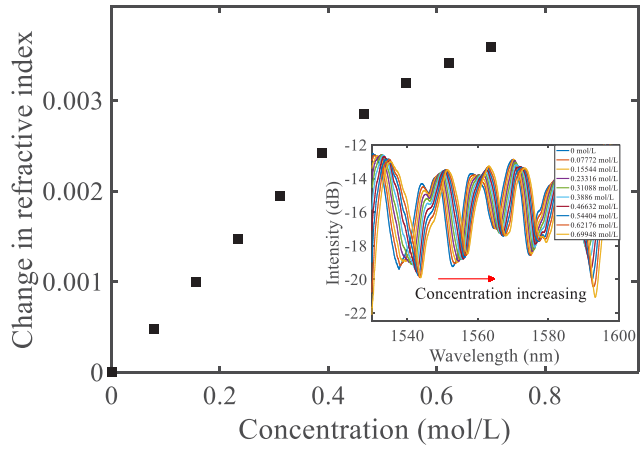


**Figure 4.** Measured changes in the refractive index derived from the OFUMOF sensor and demodulator system as a function of the solution concentration (mol/L) of nitrobenzene in ethanol. The inset includes plots of the recorded interference spectra as the concentration of nitrobenzene/ethanol solutions increases from 0 to 0.69948 mol/L in steps of 0.07772 mol/L.

the corresponding valleys) as a function of the concentration of nitrobenzene, and the inset includes a series of spectra derived from the OFUMOF sensor and demodulation system for different concentrations of nitrobenzene. The interference spectrum recorded for each concentration setting was recorded after the sensor device was immersed in the solution for 30 min. The shifts in the reflection spectra were analyzed using a cross-correlation algorithm. The spectral shifts were converted to changes in the refractive indices based on eq 3. The refractive index of the vacant MOF crystal used in the experiment is 1.39.[36] The interference spectra were red-shifted by a maximum of 4 nm when the nitrobenzene concentration increased from 0 to 0.69948 mol/L in steps of 0.07772 mol/L, corresponding to


DOI: 10.1021/acsami.8b19775
ACS Appl. Mater. Interfaces 2019, 11, 4393−4398

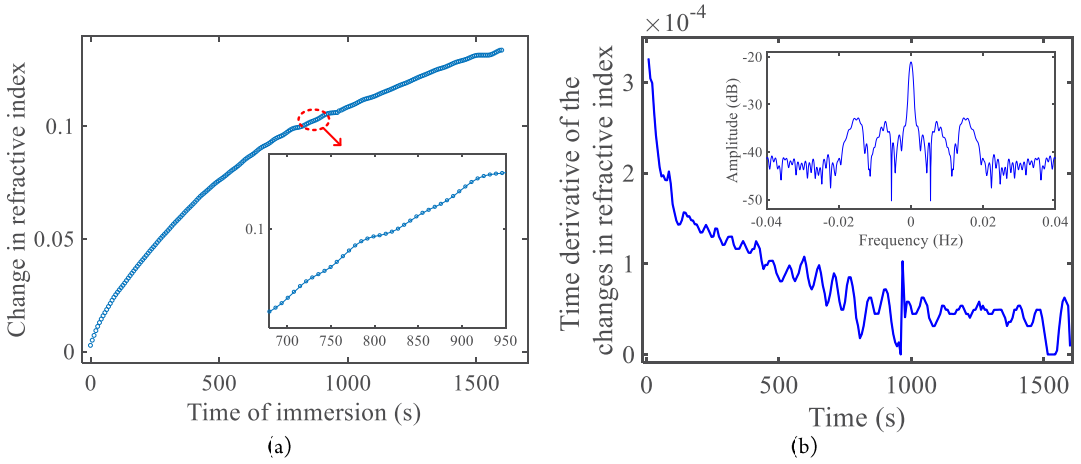


**Figure 5.** Experimental results of the sorption time profile of nitrobenzene by an HKUST-1 single crystal. (a) A plot of the change in index of refraction vs time for the adsorption of pure nitrobenzene by a single crystal of HKUST-1. The inset is an expanded view of the curve in the time range of 680 to 950 s. (b) The time derivative of the change in the refractive index data as a function of time. The inset is a plot of the Gaussian-apodized FFT of the time derivative curve.

increments of 0.003587 in the refractive indices. Because the refractive index of nitrobenzene (1.5521) is larger than that of ethanol (1.3616), as the HKUST-1 crystal adsorbed nitrobenzene from the ethanol solution, the effective refractive index of the single crystal steadily increased causing the interference spectra to shift to longer wavelengths, which matches well with our expectations. The monotonic response indicates that the proposed OFUMOF sensor structure can be used as a quantitative detection device for target chemicals after it is properly calibrated.

The sorption time profile of nitrobenzene by the HKUST-1 single crystal was investigated by immersing the sensor head into pure nitrobenzene liquid at room temperature. The OSA was controlled by a computer to record an interference spectrum every 7 s, and then a cross-correlation algorithm was applied to generate the plot of time versus spectral shift. Figure 5a shows the measured change in refractive index versus time of immersion profile adsorption curve for nitrobenzene by a single crystal of HKUST-1. The inset includes an expanded view of the curve for the time range 680 to 950 s. When the OFUMOF sensor was inserted into the nitrobenzene liquid, the molecules of nitrobenzene displaced the air inside the MOF and increased the refractive index of the MOF single crystal. As shown in Figure 5a, the refractive index of the MOF single crystal changed quickly after the sensor was initially immersed in the liquid and increased by approximately 0.1336 by the end of the adsorption experiment. Because the internal surface area within the HKUST-1 single crystal is very large compared to its geometrical external surface area, it requires some time before the nitrobenzene saturates the MOF single crystal. Interestingly, as revealed in the inset in Figure 5a, ripples were observed in the time profile adsorption curve. To further investigate this phenomenon, time derivatives were calculated from the changes in the refractive index of the MOF single crystal as a function of time. Figure 5b shows the plot of the time derivative of changes in the refractive index with respect to time, and the inset graph contains a plot of the Gaussian-apodized FFT result of the time derivative curve. The time rate of change in the refractive index of the guest/host single-crystal system dropped rapidly from an initial high rate during the first 140 s and then steadily decreased with time afterward, indicating that the uptake of the nitrobenzene molecules began rapidly and then decreased with time. Oscillations were observed in the time derivative plot, revealing that the uptake rate of the nitrobenzene molecules oscillated during the immersion period. As revealed by the FFT plot, the oscillation frequency was determined to be approximately 0.015 Hz, corresponding to a period of 67 s. Also, the harmonic (around 0.0075 Hz) with a period of 133 s was obtained in the FFT plot. More experiments are currently underway to study the detailed causes of the oscillations during the uptake of nitrobenzene molecules by the MOF single crystal.

## 4. CONCLUSIONS

We presented a device consisting of an OFUMOF sensor interfaced with a spectrum analyzer based demodulator system and a method to measure the equilibrium concentration and adsorption time profile of nitrobenzene, a chemical threat simulant, by a host single-crystal MOF. The sensing principle is based on the adsorption of guest molecules on the inner surface of the MOF HKUST-1 host, which results in changes in the overall dielectric properties (e.g., index of refraction) of the guest/host system. Measured changes in the optical interference spectra were used to determine changes in the index of refraction. The OFUMOF sensor consists of a single crystal of HKUST-1 attached to the cleaved end-face of an OF using a thin layer of epoxy. As such, the OF−MOF interface combined with the MOF−surrounding interface formed an FPI device. The changes in the dielectric properties of the molecule-guest/MOF-host single crystal system can be determined by tracking the shifts of the interference spectra derived from the FPI device. The responses of the prototype sensor to ethanol solutions of variable nitrobenzene concentrations were characterized. The results demonstrated that the OFUMOF sensor could be used as a quantitative detection device for a target chemical after proper calibration. In addition, the adsorption process of neat nitrobenzene by an HKUST-1 single crystal from the liquid phase was also monitored using the prototype sensor. The results demonstrated that our easy-to-build and inexpensive OFUMOF sensor could be used for real-time adsorption measurements of target chemicals. The HKUST-1 MOF was used in the prototype OFUMOF sensor device because single crystals can be grown to large sizes (>0.001 $mm^3$) with relative ease. HKUST-1 also has well-known chemical properties and is stable in many solvents. However, the long-term performance of the OFUMOF sensor needs to be investigated further, including the structural stability of the MOF, reusability of the single crystal, and reproducibility of the sensor output.

This work proposes and experimentally demonstrates the coupling of a highly sensitive fiber-optic interferometric probe to a porous sorbent single crystal (i.e., MOF) to form a


DOI: 10.1021/acsami.8b19775
ACS Appl. Mater. Interfaces 2019, 11, 4393−4398

chemical sensor device. Separately, neither the fiber-optic interferometer nor the MOF single crystal functions as a practical sensor because of the chemical nonspecificity of the former and the challenge in signal transduction of the latter. However, combining the prominent advantages of the two (i.e., high sensitivity and chemical selectivity) offers a universal strategy, which applies to any MOF and consequently many analytes. Moreover, the OFUMOF single crystal motif provides a portable and miniaturized probe head that is easy to fabricate and has a high potential for localized chemical detection. We anticipate that there are many approaches to fabricate the OFUMOF single-crystal structure besides using the thin adhesive layer between the OF and the MOF described herein. Although the MOF single crystal used in the present demonstration, HKUST-1, is not noted for exceptional selectivity, it is expected that MOFs that are more selective (e.g., ZIF-8) can be chosen to improve the chemical specificity of an OFUMOF single-crystal sensor for the desired chemical target. Importantly, the single crystal sensor motif provides an avenue to use polarized light to select for a chemical target guest molecule among many physisorbed guest molecules. It has been demonstrated that different guest molecules exhibit different anisotropic interactions with adsorption sites and other co-adsorbed molecules, which result in anisotropic distributions and a concomitant change in the index of refraction for the guest/host system.[37,38] Thus, it may be feasible to identify each guest molecule in a mixture of co-adsorbed guests by analyzing the changes in the polarization of the prepolarized light beam. Also, the OFUMOF single crystal based structure provides a potential scheme to probe the alignment/distribution of guest molecules in the restricted geometry of the porous host crystal using polarized light (e.g., linearly polarized). On the other hand, the polarization of the light beam output from the OFUMOF single-crystal structure will also vary with the guest type and loading, indicating that the single-crystal structure can be used as a fiber optic in-line polarizer microdevice.[38]

## AUTHOR INFORMATION


### Corresponding Authors

*E-mail: sqma@usf.edu (S.M.).
*E-mail: jieh@mst.edu (J.H.).

### ORCID

Chen Zhu: 0000-0002-3256-7330
Jason A. Perman: 0000-0003-4894-3561
Shengqian Ma: 0000-0002-1897-7069
Jie Huang: 0000-0002-8659-2910


### Author Contributions

S.M. and J.H. supervised the project and designed the experiment. C.Z. and J.A.P. performed the experiment and wrote the manuscript. C.Z., R.E.G., and J.H. analyzed the data. C.Z., J.A.P, R.E.G., S.M., and J.H. revised the manuscript.

### Author Contributions

‡These authors contributed equally.


### Funding

The work was supported by the University of Missouri Research Board, the Materials Research Center at Missouri S&T, the United States National Science Foundation (DMR-1352065), and the University of South Florida.


### Notes

The authors declare no competing financial interest.

## REFERENCES


(1) McDonagh, C.; Burke, C. S.; MacCraith, B. D. Optical Chemical Sensors. *Chem. Rev.* **2008**, *108*, 400−422.
(2) Potyrailo, R. A. Multivariable Sensors for Ubiquitous Monitoring of Gases in the Era of Internet of Things and Industrial Internet. *Chem. Rev.* **2016**, *116*, 11877−11923.
(3) Hu, Z.; Deibert, B. J.; Li, J. Luminescent Metal-Organic Frameworks for Chemical Sensing and Explosive Detection. *Chem. Soc. Rev.* **2014**, *43*, 5815−5840.
(4) Nagarkar, S. S.; Joarder, B.; Chaudhari, A. K.; Mukherjee, S.; Ghosh, S. K. Highly Selective Detection of Nitro Explosives by a Luminescent Metal−Organic Framework. *Angew. Chem., Int. Ed.* **2013**, *52*, 2881−2885.
(5) Wei, X.; Wei, T.; Xiao, H.; Lin, Y. S. Nano-Structured Pd-Long Period Fiber Gratings Integrated Optical Sensor for Hydrogen Detection. *Sens. Actuators, B* **2008**, *134*, 687−693.
(6) Zhu, C.; Zhuang, Y.; Zhang, B.; Roman, M.; Wang, P. P.; Huang, J. A Miniaturized Optical Fiber Tip High Temperature Sensor Based on Concave-Shaped Fabry−Perot Cavity. *IEEE Photonics Technol. Lett.* **2018**, *31*, 35−38.
(7) Du, Y.; Jothibasu, S.; Zhuang, Y.; Zhu, C.; Huang, J. Rayleigh Backscattering Based Macrobending Single Mode Fiber for Distributed Refractive Index Sensing. *Sens. Actuators, B* **2017**, *248*, 346−350.
(8) Zhou, H.-C.; Long, J. R.; Yaghi, O. M. Introduction to Metal−Organic Frameworks. *Chem. Rev.* **2012**, *112*, 673−674.
(9) Long, J. R.; Yaghi, O. M. The Pervasive Chemistry of Metal-Organic Frameworks. *Chem. Soc. Rev.* **2009**, *38*, 1213−1214.
(10) MacGillivray, L. R. *Metal-Organic Frameworks: Design and Application*; John Wiley & Sons: Hoboken, NJ, 2010.
(11) Farrusseng, D. *Metal-Organic Frameworks: Applications from Catalysis to Gas Storage*; John Wiley & Sons: Hoboken, NJ, 2011.
(12) Ma, S., Ed.; *Elaboration and Applications of Metal-Organic Frameworks*; World Scientific Publishing Company: Singapore, 2018.
(13) Maurin, G.; Serre, C.; Cooper, A.; Ferey, G. The New Age of MOFs and of Their Porous-Related Solids. *Chem. Soc. Rev.* **2017**, *46*, 3104−3107.
(14) Hu, Y.; Liao, J.; Wang, D.; Li, G. Fabrication of Gold NanoParticle-Embedded Metal−Organic Framework for Highly Sensitive Surface-Enhanced Raman Scattering Detection. *Anal. Chem.* **2014**, *86*, 3955−3963.
(15) Harbuzaru, B. V.; Corma, A.; Rey, F.; Jordá, J. L.; Ananias, D.; Carlos, L. D.; Rocha, J. A Miniaturized Linear pH Sensor Based on a Highly Photoluminescent Self-Assembled Europium (III) Metal−Organic Framework. *Angew. Chem.* **2009**, *121*, 6598−6601.
(16) Hromadka, J.; Tokay, B.; James, S.; Tatam, R. P.; Korposh, S. Optical Fibre Long Period Grating Gas Sensor Modified with Metal Organic Framework Thin Films. *Sens. Actuators, B* **2015**, *221*, 891−899.
(17) Lustig, W. P.; Mukherjee, S.; Rudd, N. D.; Desai, A. V.; Li, J.; Ghosh, S. K. Metal-Organic Frameworks: Functional Luminescent and Photonic Materials for Sensing Applications. *Chem. Soc. Rev.* **2017**, *46*, 3242−3285.
(18) Kreno, L. E.; Leong, K.; Farha, O. K.; Allendorf, M.; Van Duyne, R. P.; Hupp, J. T. Metal−Organic Framework Materials as Chemical Sensors. *Chem. Rev.* **2011**, *112*, 1105−1125.
(19) Lu, G.; Hupp, J. T. Metal−Organic Frameworks as Sensors: A ZIF-8 Based Fabry−Pérot Device as a Selective Sensor for Chemical Vapors and Gases. *J. Am. Chem. Soc.* **2010**, *132*, 7832−7833.
(20) Kreno, L. E.; Hupp, J. T.; Van Duyne, R. P. Metal−Organic Framework Thin Film for Enhanced Localized Surface Plasmon Resonance Gas Sensing. *Anal. Chem.* **2010**, *82*, 8042−8046.
(21) Achmann, S.; Hagen, G.; Kita, J.; Malkowsky, I. M.; Kiener, C.; Moos, R. Metal-Organic Frameworks for Sensing Applications in the Gas Phase. *Sensors* **2009**, *9*, 1574−1589.
(22) Allendorf, M. D.; Houk, R. J. T.; Andruszkiewicz, L.; Talin, A. A.; Pikarsky, J.; Choudhury, A.; Gall, K. A.; Hesketh, P. J. Stress-Induced Chemical Detection Using Flexible Metal−Organic Frameworks. *J. Am. Chem. Soc.* **2008**, *130*, 14404−14405.



DOI: 10.1021/acsami.8b19775
*ACS Appl. Mater. Interfaces* 2019, 11, 4393−4398

(23) Zybaylo, O.; Shekhah, O.; Wang, H.; Tafipolsky, M.; Schmid, R.; Johannsmann, D.; Wöll, C. A Novel Method to Measure Diffusion Coefficients in Porous Metal-Organic Frameworks. *Phys. Chem. Chem. Phys.* **2010**, *12*, 8093−8098.
(24) Ma, D.; Li, B.; Zhou, X.; Zhou, Q.; Liu, K.; Zeng, G.; Li, G.; Shi, Z.; Feng, S. A Dual Functional MOF as a Luminescent Sensor for Quantitatively Detecting the Concentration of Nitrobenzene and Temperature. *Chem. Commun.* **2013**, *49*, 8964−8966.
(25) Chong, X.; Kim, K.-J.; Li, E.; Zhang, Y.; Ohodnicki, P. R.; Chang, C.-H.; Wang, A. X. Near-Infrared Absorption Gas Sensing with Metal-Organic Framework on Optical Fibers. *Sens. Actuators, B* **2016**, *232*, 43−51.
(26) Chong, X.; Kim, K.-J.; Li, E.; Zhang, Y.; Ohodnicki, P. R.; Chang, C.-H.; Wang, A. X. Ultra-Sensitive CO2 Fiber-Optic Sensors Enhanced by Metal-Organic Framework Film. *CLEO: Science and Innovation*, San Jose, CA, June 5−10, 2016, DOI: 10.1364/CLEO_AT.2016.JTu5A.138 .
(27) Kim, K. J.; Lu, P.; Culp, J. T.; Ohodnicki, P. R. Metal−Organic Framework Thin Film Coated Optical Fiber Sensors: A Novel Waveguide-Based Chemical Sensing Platform. *ACS Sens.* **2018**, *3*, 386−394.
(28) Nazari, M.; Forouzandeh, M. A.; Divarathne, C. M.; Sidiroglou, F.; Martinez, M. R.; Konstas, K.; Muir, B. W.; Hill, A. J.; Duke, M. C.; Hill, M. R.; Collins, S. F. UiO-66 MOF End-face-Coated Optical Fiber in Aqueous Contaminant Detection. *Opt. Lett.* **2016**, *41*, 1696−1699.
(29) Wei, T.; Han, Y.; Li, Y.; Tsai, H. L.; Xiao, H. Temperature-Insensitive Miniaturized Fiber Inline Fabry-Perot Interferometer for Highly Sensitive Refractive Index Measurement. *Opt. Express* **2008**, *16*, 5764−5769.
(30) Zhang, J.; Dong, J.; Luo, M.; Xiao, H.; Murad, S.; Normann, R. A. Zeolite-Fiber Integrated Optical Chemical Sensors for Detection of Dissolved Organics in Water. *Langmuir* **2005**, *21*, 8609−8612.
(31) Li, L.; Sun, F.; Jia, J.; Borjigin, T.; Zhu, G. Growth of Large Single MOF Crystals and Effective Separation of Organic Dyes. *CrystEngComm* **2013**, *15*, 4094−4098.
(32) Lichtfouse, E., Schwarzbauer, J., Robert, D., Eds.; *Pollutant Diseases, Remediation and Recycling*; Springer: New York, 2013.
(33) Kazak, C.; Yilmaz, V. T.; Yazicilar, T. K. trans-Bis-(ethylenediamine)bis(p-nitrobenzoxasulfamato)copper(II). *Acta Crystallogr., Sect. E: Crystallogr. Commun.* **2004**, *60*, m593−m595.
(34) Abourahma, H.; Bodwell, G. J.; Lu, J.; Moulton, B.; Pottie, I. R.; Walsh, R. B.; Zaworotko, M. J. Coordination Polymers from Calixarene-Like [Cu2(Dicarboxylate)2]4 Building Blocks: Structural Diversity via Atropisomerism. *Cryst. Growth Des.* **2003**, *3*, 513−519.
(35) Moulton, B.; Lu, J.; Hajndl, R.; Hariharan, S.; Zaworotko, M. J. Crystal Engineering of a Nanoscale Kagomé Lattice. *Angew. Chem., Int. Ed.* **2002**, *41*, 2821−2824.
(36) Redel, E.; Wang, Z.; Walheim, S.; Liu, J.; Gliemann, H.; Wöll, C. On the Dielectric and Optical Properties of Surface-Anchored Metal-Organic Frameworks: A Study on Epitaxially Grown Thin Films. *Appl. Phys. Lett.* **2013**, *103*, 091903.
(37) Greenaway, A.; Gonzalez-Santiago, B.; Donaldson, P. M.; Frogley, M. D.; Cinque, G.; Sotelo, J.; Moggach, S.; Shiko, E.; Brandani, S.; Howe, R. F.; Wright, P. A. In situ Synchrotron IR Microspectroscopy of CO2 Adsorption on Single Crystals of the Functionalized MOF Sc2 (BDC-NH2) 3. *Angew. Chem., Int. Ed.* **2014**, *53*, 13483−13487.
(38) Auerbach, S. M.; Carrado, K. A.; Dutta, P. K. *Handbook of Zeolite Science and Technology*; CRC Press: Boca Raton, FL, 2013.


DOI: 10.1021/acsami.8b19775
*ACS Appl. Mater. Interfaces* 2019, 11, 4393−4398